Chemical Engineering Journal 99 (2004) 145–152

Chemical Engineering Journal

www.elsevier.com/locate/cej

Experimental analysis of a corrugated plate photocatalytic reactor

Zisheng Zhang [b], William A. Anderson [a,*], Murray Moo-Young [a]

[a] *Department of Chemical Engineering, University of Waterloo, Waterloo, Ont., Canada N2L 3G1*
[b] *Department of Chemical Engineering, University of Ottawa, Ottawa, Ont., Canada*

Abstract

A corrugated plate reactor configuration was developed and assessed using 4-chlorophenol degradation experiments and mass transfer tests. Two other reactor systems, a flat plate reactor and a slurry reactor, were examined for comparative purposes. The corrugated plate reactor was found to be up to 150% faster and more energy-efficient than a similar flat plate reactor. Its electrical energy per order of concentration reduction (EE/O) was estimated to be as low as 37 kWh/m^3 and was close to that of a slurry system. Mass transfer rates in corrugated plate reactors were found to be up to 600% higher than those in the flat plate reactor. The superior performance of this reactor is due primarily to its large illuminated catalyst surface area per unit volume, and its ability to effectively deliver both photons and reactants to the catalyst surfaces.

Keywords: Corrugated plate; Photocatalytic reactor; Mass transfer; Photocatalysis

1. Introduction

Research into photocatalysis has been very active for the last two decades due to the potential use of this heterogeneous photochemical process in water and air decontamination. Degradation of different substances, reaction mechanisms and kinetics, activities of different catalysts, and effects of selected environmental conditions have been studied extensively and many photoreactor systems have been examined.

Despite all the previous work, a commercially competitive full-scale photocatalytic water treatment system has not yet been widely accepted in practice. The major barrier for photocatalysis to obtain wider industrial acceptance is its high cost as well as its low overall rate and low energy efficiency due, among other factors, to the low-order dependency (usually between 0.5 and 1) of reaction rates on radiation intensity and limited capacity to deliver photons; reactants to catalyst surfaces [1]. Superior catalysts, more efficient light sources, or novel photoreactors are required in order for photocatalysis to become more cost-effective and to gain wider industrial application.

The objective of this work was to experimentally examine the performance of an alternative immobilized TiO_2 reactor design, which theoretically has advantages in terms of catalyst surface area per unit volume, as well as photon capture and distribution on the catalyst surface [2]. Degradation of 4-chlorophenol was conducted for the purpose of reactor performance evaluation. Two other reactor systems, a flat plate reactor and a slurry reactor, were examined for comparative purposes. Mass transfer rates between the bulk stream and the catalyst films were measured for comparison with the observed reaction rates.

1.1. Corrugated plate photocatalytic reactor

As a result of the low-order dependency of photocatalytic reaction rates on the radiation intensity and the UV absorption characteristics of TiO_2 films [3], an effective and energy-efficient photoreactor must possess: (1) a large illuminated catalyst surface area per unit reactor volume; (2) satisfactory mass transfer capacity between the main stream and the surfaces of catalyst films; (3) the capability for the catalyst film to recapture reflected photons; (4) a high efficiency in converting electricity to ultraviolet light. These requirements are in addition to those desired for any process systems, such as low capital, operating, and maintenance costs, good reliability and operating resilience, and minimum demand for up- and down-stream treatment steps.

Fig. 1 is a sketch of the reactor used in this study. A scaled-up version would employ multiple plates in parallel, with the catalyst was immobilized and illuminated on both sides of the corrugated plates. A corrugated plate could also be illuminated conveniently on one side with sunlight. The

Abbreviations: 4CP, 4-chlorophenol; BA, benzoic acid; EE/O, electrical energy per order (kWh/m^3); HPLC, high performance liquid chromatography; TOC, total organic carbon

* Corresponding author. Tel.: +1-519-888-4567; fax: +1-519-746-4979.
E-mail address: wanderson@uwaterloo.ca (W.A. Anderson).

1385-8947/$ – see front matter © 2004 Elsevier B.V. All rights reserved.
doi:10.1016/j.cej.2004.01.001

Nomenclature

A	total illuminated area of the immobilized catalyst film (m^2)
C	bulk concentration of 4-chlorophenol (mg/l)
C_f	final bulk concentration of 4-chlorophenol (mg/l)
C_s	average concentration of 4-chlorophenol on catalyst film (mg/l)
C_0	initial bulk concentration of 4-chlorophenol (mg/l)
D_{4CP}	diffusivity of 4-chlorophenol in water (m^2/h)
D_{O_2}	diffusivity of oxygen in water (m^2/h)
I	radiation intensity before penetrating the lamp sleeve (W/m^2)
k_L	measured average mass transfer coefficient (m/h)
K	apparent reaction rate constant (l/mg)
K_0	empirical model parameter (g/m^2 h)
O	bulk aqueous concentration of oxygen (mg/l)
O_S	average concentration of oxygen on catalyst film (mg/l)
P	total power input (kW)
t	run time (h)
V	total volume of the reaction medium (m^3)
V_R	total reactor volume (m^3)

illuminated catalyst film area in a corrugated plate reactor could be very high, depending on the dimensions of the corrugated plate used. Listed in Table 1 are the illuminated catalyst surface areas of the corrugated plate reactor and of a few other reactor configurations for comparison. Only the tube light reactor [4] possesses an illuminated catalyst film area that is higher than those of the corrugated plate reactors. In addition, the opposing catalyst surfaces in the corrugated plate reactor offer a mechanism for capture of photons which are initially reflected from the surface [2].

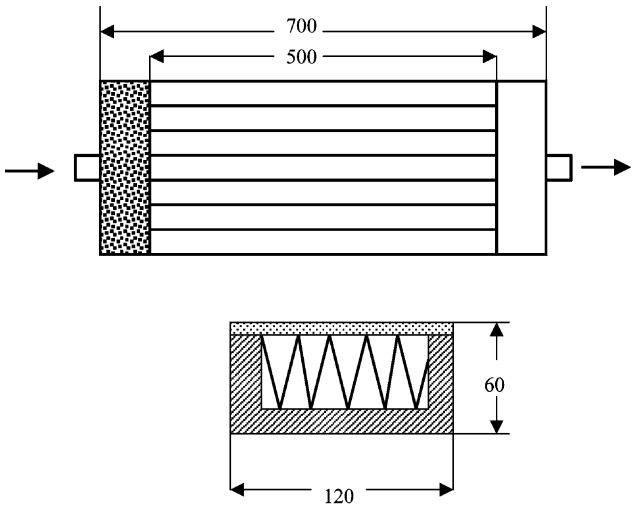

Fig. 1. Schematic of the experimental corrugated plate reactor, with dimensions in mm. Top view shows flow direction and packed bed flow distributor. A cross-section shows the corrugated plate and the UV transparent cover on top, through which the illumination was applied.

2. Experimental methods and materials

2.1. Chemicals and catalyst

Reagent grade 4-chlorophenol (4CP) from BDH Ltd., UK, was used as the model pollutant. Analytical grade methanol and acetonitrile from BDH Inc., Canada, were used during HPLC analysis. Concentrated hydrochloric acid from BDH Inc., Canada, was used to clean the corrugated plates before catalyst immobilization. The water used for all the runs was deionized water filtered with a Milli-Q system. Degussa P25 TiO_2 was used as the catalyst, either suspended in water or immobilized on stainless steel plates. A procedure for the immobilization of TiO_2 on stainless steel plate was developed based on information from the literature [6,7]. The plate was cleaned with 20% HCl then dried at 200 °C for 2 h. A 180 g/l slurry of TiO_2 was created in 25% aqueous

Table 1
TiO_2 film area per unit reactor volume for selected reactors

Reactor configuration	A/V_R (m^2/m^3)	Notes
Tube light reactor[a]	>1000	Based on [5]; catalyst immobilized on the walls of the lamps; lamps take 75% of the reactor volume
Multiple tube reactor[b,c]	up to 45	Reactor structure based on [4]; assumed distance between lamp-sleeve assembly: 0.01 m; catalyst immobilized on outer wall of the lamp sleeves
Packed bed reactor[b,c]	up to 80	Assumed distance between the lamp-sleeve assembly: 0.01 m; catalyst immobilized on spherical packing, 1 cm diameter.
Flat plate	≈26	
CP reactor (angle 20°)	up to 115	Reactor structure shown in Fig. 1; catalyst immobilized on the surfaces of the corrugated plates; height of plate is 5 cm.
CP reactor (angle 14°)	up to 165	
CP reactor (angle 10°)	up to 230	
CP reactor (angle 7°)	up to 330	

[a] Special lamps with a diameter of 0.0045 m in direct contact with contaminated water.
[b] Assumed illumination source: regular tubular lamp with a diameter of 0.036 m.
[c] Exterior diameter of the lamp sleeve: 0.056 m.

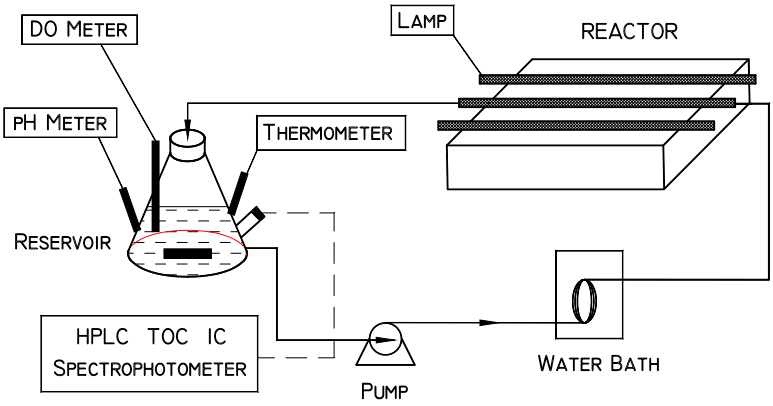

Fig. 2. Schematic of the experimental system setup.

methanol, and this was painted onto the plate surface in a thin coating. The plate was then dried at 300 °C for about 5 h, and gently rinsed after cooling.

2.2. Photoreactor and system setup

Fig. 2 shows the experimental system setup. Illumination was provided with three 40 W fluorescent lamps (Philips, TLK 40W/10R) placed above the reactor and in parallel with the lamp sleeve. These lamps emit in UV-A range, with an average wavelength of 353 nm. The pump was a centrifugal magnetically coupled type and all the water-contacting parts were made from polypropylene. The reservoir was made from a 1000 ml Erlenmeyer flask with ports for inlet, outlet, sampling, pH probe, dissolved oxygen (DO) probe, and thermometer. Oxygen required for the reactions was admitted into the reservoir through an opening to the ambient air. The reservoir inlet was built to be tangential to its wall so that sufficient air could be entrained through the water/air interface. This allowed the dissolved oxygen level in the reaction medium to be constant at approximately 7.0 mg/l during all the experimental runs. The temperature was controlled at 26.5 °C with a water bath.

The corrugated plate reactor (Fig. 1) consisted of an acrylic chamber, a distributor, and a TiO_2-coated corrugated plate, fabricated by bending 1.2 mm stainless steel sheets to predetermined corrugation angles, with an overall height and width of 50 and 80 mm, respectively. The light transmitting reactor wall was made from a UV-A transmitting Plexiglas (G-UVT). A stainless steel screen enclosure packed with 5 mm glass beads was used as the water distributor in the entrance zone of the plastic chamber (before the reaction zone). The flat plate reactor consisted of the same plastic chamber, the distributor, and a TiO_2-coated flat plate in the chamber placed 2.5 cm from the light transmitting wall. The dimension of the catalyst coating was 80 mm by 500 mm. The plate was made from 3/64 in. stainless steel sheets (SS-314). The slurry system was formed when the artificial wastewater was spiked with 1 g/l of TiO_2, and circulated through the same plastic chamber, in the absence of a coated stainless steel sheet.

2.3. Experimental procedure

Before each experimental run, the reactor system was cleaned by pumping deionized water through it for about 10 min without illumination. As indicated by the optical densities of the water, this procedure allowed the removal of any residual compounds from previous runs. The system was then drained and 4 l of premixed 30 mg/l 4CP solution was introduced. This solution was pumped through the system for 1–5 min and then the lamps were switched on to initiate the reaction. Samples were then taken from the reservoir at different times and analyzed for UV absorbance at 224 nm, for composition, and for total organic carbon. All the samples were analyzed without any pretreatment except for those from the slurry reactor, which were centrifuged at a speed of 6000 rpm for 10 min to remove the TiO_2 particles before analysis.

2.4. Analysis methods

UV absorbance of the samples was measured using a UV/Vis spectrophotometer (Genesys 2, Milton Roy). Composition of the reaction medium was determined with an HPLC system, consisting of an LKB Bromma 2249 gradient pump, a Gilson Model 401 diluter, a Gilson Model 231 sample injector, a Regis ODS II reversible column (15 cm × 4.6 mm i.d., 5 μm), and a Gilson Model 116 UV detector, with peak integration performed on a spectra-physics SP4270 integrator. The eluent contained 45% water, 50% methanol, and 5% acetonitrile and was pumped isocratically through the system at a flowrate of 0.5 ml/min. The detector was set at 225–230 nm with sensitivities of 0.05–0.1 AUFS. TOC (TC-IC) was determined with an Astro 2001 UV-persulphate TOC analyzer or a combustion-type TOC analyzer with an infrared detector (TOC-500, Shimadzu Corporation, Japan). Radiation intensity on the lamp sleeve was determined with a Spectroline digital radiometer

(DRC-100X, Spectronics Corporation, New York) equipped with a DIX-365 sensor. The microstructures of the catalyst films were observed under a scanning electron microscope manufactured by Joel Ltd., Japan.

2.5. Mass transfer measurement

The benzoic acid dissolution method was adopted [8] for the mass transfer experiments from the surface of flat and corrugated plates. Reagent grade benzoic acid (BDH Inc., Toronto) was coated on a stainless steel sheet of the desired geometry with a known area, and tap water was pumped through the reactor (lamps off) in a once-through mode at a variety of flowrates. The benzoic acid concentration in the effluent was determined by measuring the UV absorbance of the sample at 226 nm and comparing it with a calibration curve. During all mass transfer experimental runs, the water temperature was kept constant at 26.5 °C. Steady-state concentration data was used in a mass balance to determine the mass transfer rates and average coefficients from the following equation:

$$C^{\text{out}}Q = \bar{k}_{\text{L}} A \frac{(C^* - C^{\text{in}}) - (C^* - C^{\text{out}})}{\ln\left((C^* - C^{\text{in}})/(C^* - C^{\text{out}})\right)}$$

3. Results and discussion

3.1. System validation

Before the start of degradation experiments, the effect of photolysis and catalysis on 4CP concentration profile was tested and found to be negligible. Dye tracer tests were also performed and the velocity profile in the reactor was found to be close to plug flow by visual observation. The opacity of the film was examined by painting the same slurry onto a UV transmitting acrylic plate and measuring the UV transmission with the radiometer. Two blank runs were also carried out in the flat plate reactor using deionized water at two typical flowrates. The UV absorbance of the samples at 300 nm was found to be constant at zero during the course of these runs, indicating that the catalyst film was mechanically stable.

The average catalyst weight per unit immobilized surface area was evaluated by weighing the plate before and after immobilization and was found to be about 1 mg TiO_2/cm^2 of the coating. The microstructure of immobilized typical catalyst films was observed under a scanning electron microscope. Based on the density and the mass balance of the catalyst, the thickness and the porosity of the film were estimated to be around 10 μm and 80%, respectively.

3.2. Experimental results

Typical experimental results are plotted Figs. 3–7. During the course of a typical degradation run, the pH of the reaction medium dropped from an initial value of around 6.0 to about 3.8 near the completion of the reaction. HPLC chromatograms showed five UV-absorbing reaction intermediates. The result of a mass balance indicated that the total organic carbon (TOC) attributable to the intermediates was much lower than that due to the parent compound during most of the experimental run time, which agrees with previous studies [9–12]. The fitted lines in Figs. 3–6 were generated with the parameters obtained by fitting a Langmuir–Hinshelwood type of empirical relationship, as

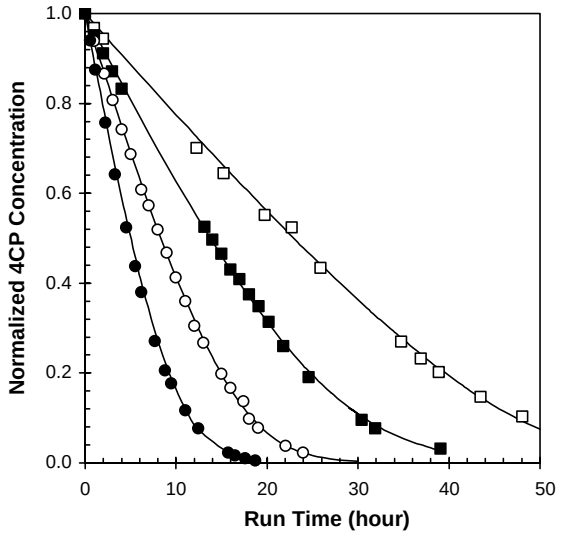

Fig. 3. Effect of Reynolds number on degradation kinetics: flat plate reactor flat plate; $C_0 = 30$ mg/l; $I = 122$ W/m^2; (□) $Re = 431$; (■) $Re = 782$; (○) $Re = 1633$; (●) $Re = 5813$; lines: fittings.

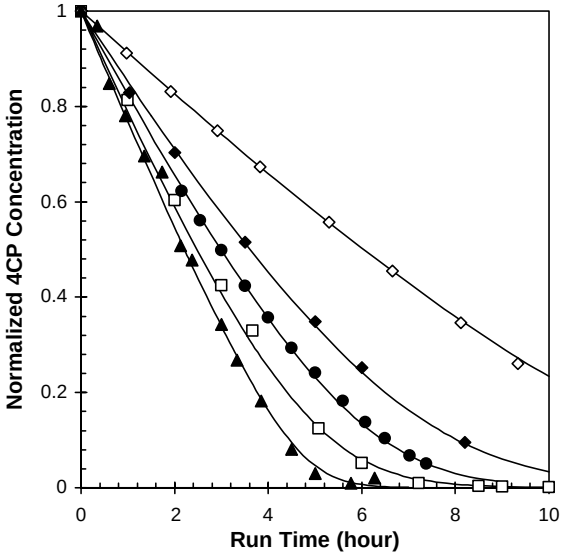

Fig. 4. Comparison of 4CP degradation in flat, slurry and corrugated plate reactors: 4CP concentration profiles: flowrate = 23 l/min; $C_0 = 30$ mg/l; $I = 122$ W/m^2; (□) angle = 7°; (●) angle = 20°; (◆) angle = 40°; (◇) flat plate reactor; (▲) slurry reactor; lines: fittings.

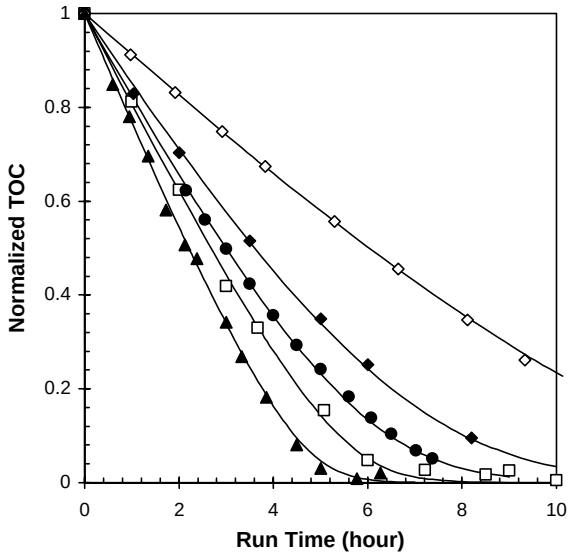

Fig. 5. Comparison of 4CP degradations in flat, slurry and corrugated plate reactors: total organic carbon profiles: flowrate = 23 l/min; $C_0 = 30$ mg/l; $I = 122$ W/m^2; (□) angle = 7°; (●) angle = 20°; (◆) angle = 40°; (◇) flat plate reactor; (▲) slurry reactor; lines: fittings.

expressed in Eqs. (1) and (2) below:

$$\frac{V}{A}\frac{dC}{dt} = -\frac{K_0 KC}{1+KC} \quad (1)$$

$$C = C_0 - \frac{1}{K}\ln\frac{C}{C_0} - \frac{A}{V}K_0 t \quad (2)$$

These fitted lines are useful for interpolation and extrapolation to some extent, but K and K_0 are not intrinsic kinetic parameters, since they are affected by mass transfer and light intensity effects. Intrinsic parameters have been obtained through more rigorous models incorporating these effects [13].

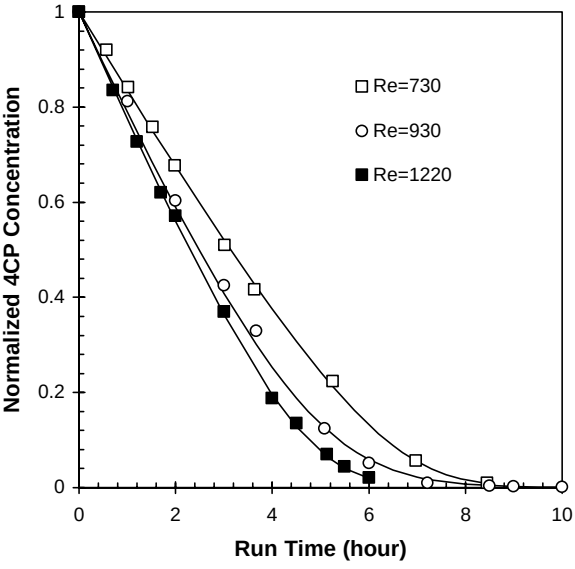

Fig. 6. Effect of Reynolds number on degradation kinetics: corrugated plate reactor angle = 7°; $C_0 = 30$ mg/l; $I = 122$ W/m^2; (□) $Re = 730$; (○) $Re = 930$; (■) $Re = 1220$; lines: fittings.

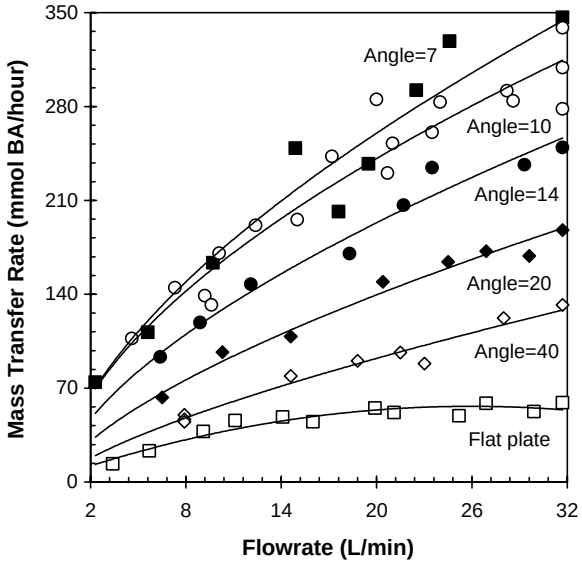

Fig. 7. Overall mass transfer rates from a flat plate and corrugated plates with different angles markers: data; lines: best fittings; (□) flat plate; (■) angle = 7°; (○) angle = 10°; (●) angle = 14°; (◆) angle = 20°; (◇) angle = 40°.

Fig. 7 shows the average overall mass transfer rates in the flat and corrugated plate reactors as a function of Reynolds number. In these measurements, a single corrugated channel was coated and used to measure mass transfer, and the results were extrapolated to the total area. Since the smaller angles have more channels, this extrapolation results in a higher apparent scatter in the data as the angle decreases.

Figs. 8 and 9 depict the normalized average concentrations of 4-chlorophenol and oxygen on the surface of the catalyst films. The curves in these two figures were ob-

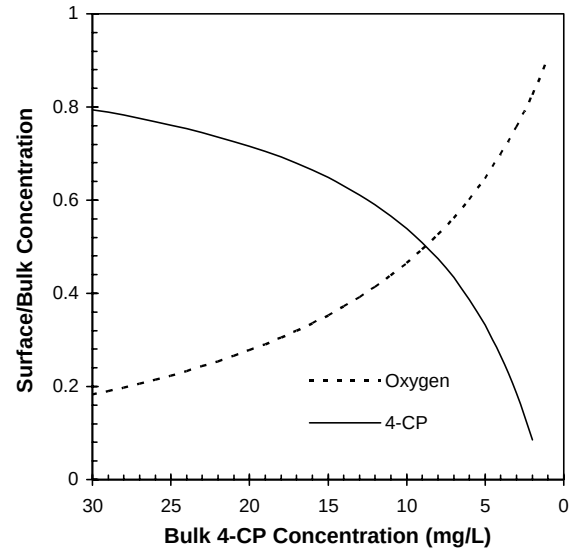

Fig. 8. Relative surface concentrations of reactants during 4CP degradation in a flat plate reactor $I = 122$ W/m^2; $C_0 = 30$ mg/l; $Re = 4313$.

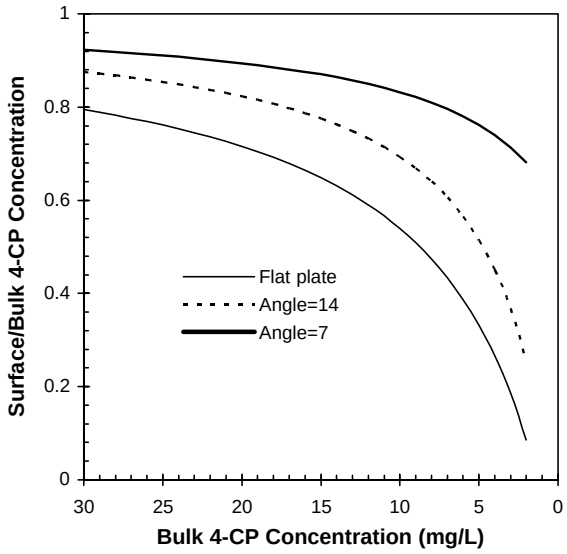

Fig. 9. Surface concentration profiles of 4CP during degradation in flat and corrugated plate reactors: $I = 122\,\mathrm{W/m^2}$; $C_0 = 30\,\mathrm{mg/l}$; flowrate = 23 l/min.

tained using Eqs. (3) and (4), which were derived based on a mass balance, two-film mass transfer theory, and the reaction stoichiometry, assuming all the reaction intermediates were negligible:

$$\frac{C_S}{C} = 1 - \frac{V}{k_L A C}\frac{dC}{dt} \tag{3}$$

$$\frac{O_S}{O} = 1 - \frac{416}{257}\left(\frac{D_{4CP}}{D_{O_2}}\right)^{2/3}\frac{V}{k_L A O}\frac{dC}{dt} \tag{4}$$

3.3. Effect of mass transfer

Figs. 3 and 6 show the effect of Reynolds number on the kinetics of 4CP degradation in the flat plate and a corrugated plate reactor. The Reynolds number was determined based on the hydraulic radius [14] of a triangular cross-section channel. The results in these two figures indicate that the reactions in both reactors were limited by mass transfer. It is interesting to note from Fig. 3 that deviations from zero-order kinetics occur at approximately the same 4CP concentration, although the Reynolds number and therefore the mass transfer rates were different. This occurs because the reaction rate is affected by transfer of both 4CP and oxygen (two reactants) to the catalytic surface. Since the 4CP concentration was initially much higher than that of oxygen (7 mg/l), the process was actually limited by the transfer of oxygen until the concentration of 4CP was reduced to such a level that the ratio of their mass transfer rates is equal to the stoichiometrically defined one. Based on available correlations [14,15] and the diffusivities of these two substances, this corresponds to a 4CP concentration of around 8.7 mg/l. Since the oxygen concentration was kept constant, the degradation should therefore follow zero-order kinetics with respect to 4CP when its concentration is higher than about 8.7 mg/l, and change gradually to first order as the reaction proceeds further. The results in Fig. 8 agree well with this estimation.

3.4. Reactor performance comparison

The performances of the flat plate, the slurry, and the corrugated plate reactors in 4-chlorophenol degradation are summarized in Fig. 4 (in terms of 4CP concentration) and Fig. 5 (in terms of the TOC of the reaction medium). Based on the results in these two figures, we find that the best corrugated plate reactor (7° angle), was approximately 150% faster and therefore more energy-efficient than the flat plate reactor. The degradation rates in the corrugated plate and slurry reactors were similar.

The degradation in the slurry reactor was approximately twice as fast as that in the flat plate reactor, which agrees with one previous observation [16]. This is due to the enormous difference of the illuminated catalyst surface area between the two systems. Based on the loading, the density, and the size of the catalyst particle aggregates [4], the illuminated surface area of the catalyst aggregates in the slurry was estimated to be up to 260 times the surface area in the flat plate reactor. A linear relationship between surface area and rates would not be expected, due to significant UV scattering and absorption effects in the slurry reactor [17].

As shown in Fig. 7, the overall mass transfer rates in corrugated plate reactors are up to six-fold higher that those in the flat plate reactor, depending on the angle of the corrugated plate and water flowrate.

3.5. Effect of corrugated plate angle

As can be seen from Figs. 4 and 5 that the performance of a corrugated plate reactor is strongly dependent on the angle of the corrugated plate. Within the range of the angles examined, the smaller the angle, the more efficient the system. This result is understandable since reactors packed with corrugated plates with small angles offer higher mass transfer capacities (Fig. 7) and larger areas of the illuminated catalyst films (Table 1). In addition, it has been shown that corrugated plates with small angles can also capture a larger fraction of the reflected photons [2].

3.6. Energy efficiency

As a method of estimating the energy efficiencies of the processes in which light is an input, electrical energy per order (EE/O) has been used widely [18]. The EE/O is defined as the electrical energy (in KWh) required to mineralize the pollutant in $1\,\mathrm{m^3}$ of contaminated water by one order of magnitude (Eq. (5)). Generally, the higher the energy efficiency of a system, the lower the EE/O. For reactions with first order kinetics, the EE/O offers an unbiased evaluation of the energy efficiency of a reactor system. For reactions with other types of kinetics, the EE/O becomes a function

Table 2
Reported energy efficiencies of several reactor configurations [21–24]

Reactor, illumination source, compound	Initial concentration (mg/l)	EE/O (kWh/m^3)	References
Annular slurry, fluorescent lamp, phenol	94	106	21
Spiral glass coil, fluorescent lamp, 4CP	1.3	74[a]	22
Spiral glass coil, fluorescent lamp, phenol	76	360	19
Fibre optics bundle, high pressure mercury, 4CP	13	25000	23
Fluidized bed, medium pressure mercury, 4CP and *p*-toluenesulfonic acid	64 each	9300	24
Annular slurry, fluorescent lamp, 4CP	32	155	20
Flat plate, fluorescent lamp, 4CP		93	[b]This work
CP reactor, fluorescent lamp, 4CP	30	37	
Slurry reactor, fluorescent lamp, 4CP		32	

[a] Tygon tubing was used, potentially affecting the results through absorption.
[b] A lamp energy efficiency of 17% was assumed.

of the initial pollutant concentration and can only be used for rough estimation purposes:

$$\mathrm{EE/O} = \frac{Pt}{V \log (C_0/C_\mathrm{f})} \quad (5)$$

Table 2 shows the calculated EE/O values based on this and previous research on the degradation of chlorinated phenols. Although the photocatalytic degradability of all phenolic compounds is comparable on a carbon basis [19], these values can only be used as a rough guide to the effectiveness of the reactor systems examined, due to the inconsistency of the experimental conditions in different studies. As can be seen from this table, the corrugated plate reactor offered the best energy efficiency.

Based on the model-determined photon absorption rates [2], the initial quantum efficiencies of the flat as well as the corrugated plate reactors (7° angle) were calculated. They are both lower than 1%. Since 26 hydroxyl radicals are required to mineralize each 4CP molecule [20], the upper limit of the quantum efficiency for 4CP degradation is estimated to be 3.85%. Therefore, more than 70% of the photo-generated hydroxyl radicals were dissipated as waste in the systems examined in this study, which is a typical result for photocatalytic reactors.

4. Conclusions

The corrugated plate reactor was found to be up to 150% faster and more energy-efficient than the flat plate reactor for the degradation of 4CP. Its EE/O was estimated to be 37 kWh/m^3 and was close to that of the slurry system examined. These experimental results, together with an expected low capital, operating, and maintenance cost, and good scale-up potential of this reactor indicate the potential of the design.

The superior performance of the corrugated plate reactor is due primarily to its large illuminated catalyst surface area and its capacity for transport of reactants and efficient capture of photons on the catalyst surfaces. Within the flowrate range examined, the corrugated plate reactor showed an enhancement of overall mass transfer rates of up to 400–600% over that of the flat plate reactor.

Photocatalysis on immobilized TiO_2 films can be limited by the transfer of either the oxidant (i.e. oxygen) or the substances being oxidized (i.e. 4CP) between the reaction sites and the bulk flow stream. Based on the experimental results, the photocatalytic reactions in the flat plate reactor were initially limited by oxygen transfer, but shifted to 4CP transfer limitations as the reactions proceeded.

Acknowledgements

Financial support for this work was provided by the Natural Science and Engineering Research Council of Canada. Z. Zhang was the holder of an Ontario Graduate Scholarship during part of this work.

References

[1] Y. Parent, D. Blake, B.K. Magrini, C. Lyons, C. Turchi, A. Watt, E. Wolfrum, M. Prairie, Solar photocatalytic processes for the purification of water: state of development and barriers to commercialization, Solar Energy 56 (1996) 429.
[2] Z. Zhang, W.A. Anderson, M. Moo-Young, Rigorous modeling of UV absorption by TiO_2 films in a photocatalytic reactor, AIChE J. 46 (2000) 1461.
[3] J.C. Crittenden, Y. Zhang, D.W. Hand, D.L. Perram, Destruction of organic compounds in water using fixed bed photocatalysts, Int. Solar Energy Conf. 1 (1995) 449.
[4] A.K. Ray, A.C.M. Beenackers, Development of a new photocatalytic reactor for water purification, Catal. Today 40 (1998) 73.
[5] A.K. Ray, New photocatalytic reactors for destruction of toxic water pollutants, Dev. Chem. Eng. Miner. Process. 5 (1997) 115.
[6] H.I. De Lasa, J. Valladares, Photocatalytic reactor, US Patent 5,683,589 (1997).
[7] J. Pacheco, A.S. Watt, C.S. Turchi, Solar detoxification of water: outdoor testing of prototype photoreactors, ASME—Solar Energy (1993) 43.
[8] P. Harriott, R.M. Mamilton, Solid–liquid transfer in turbulent pipe flow, Chem. Eng. Sci. 20 (1965) 1073.

[9] M. Lindner, J. Theurich, D.W. Bahnemann, Photocatalytic detoxification of organic compounds: accelerating the process efficiency, Wat. Sci. Technol. 35 (1997) 79.
[10] U. Stafford, K.A. Gray, P.V. Kamat, Photocatalytic degradation of 4-chlorophenol: a mechanistically-based model, Res. Chem. Intermed. 23 (1997) 355.
[11] H. Al-Ekabi, N. Serpone, E. Pelizzetti, C. Minero, M.A. Fox, R.B. Draper, Kinetic studies in heterogeneous photocatalysis 2: TiO_2-mediated degradation of 4-chlorophenol alone and in a three component mixture of 4-chlorophenol, 2,4-dichlorophenol, and 2,4,5-trichlorophenol in air equilibrated aqueous media, Langmuir 5 (1989) 250.
[12] G. Al-Sayyed, J.C. D'Oliveira, P. Pichat, Semiconductor-sensitized photodegradation of 4-chlorophenol in water, J. Photochem. Photobiol. A: Chem. 58 (1991) 99.
[13] Z. Zhang, W.A. Anderson, M. Moo-Young, Modeling of corrugated plate photocatalytic reactors and experimental validation, Chem. Eng. Sci. 58 (2003) 911.
[14] W.L. McCabe, J.C. Smith, P. Harriott, Unit Operations of Chemical Engineering, 5th ed., McGraw-Hill, New York, 1993.
[15] P.H. Calderbank, M. Moo-Young, The continuous phase heat and mass transfer properties of dispersions, Chem. Eng. Sci. 16 (1961) 39.
[16] R.J. Enzweiler, D.L. Mowery, L.M. Wagg, J.J. Dong, Pilot scale investigation of photocatalytic detoxification of BETX water, Int. Solar Energy Conf. (1994) 155.
[17] A.E. Cassano, O.M. Alfano, Reaction engineering of suspended solid heterogeneous photocatalytic reactors, Catal. Today 58 (2000) 167–197.
[18] J.R. Bolton, K.G. Bircher, W. Tumas, C.A. Tolman, Figures of merit for the technical development and applications of advanced oxidation processes, J. Adv. Oxid. Technol. 1 (1996) 13.
[19] H. Al-Ekabi, N. Serpone, Kinetic studies in heterogeneous photocatalysis. 1. Photocatalytic degradation of chlorinated phenols in aerated aqueous solutions over TiO_2 supported on a glass matrix, J. Phys. Chem. 92 (1988) 5726.
[20] U. Stafford, K.A. Gray, P.V. Kamat, Photocatalytic degradation of 4-chlorophenol: the effects of varying TiO_2 concentration and light wavelength, J. Catal. 167 (1997) 25.
[21] K. Okamoto, Y. Yamamoto, H. Tanaka, M. Tanaka, A. Itaya, Heterogeneous photocatalytic decomposition of phenol over TiO_2 powder, Bull. Chem. Soc. Jpn. 58 (1985) 2015.
[22] R.W. Matthews, Solar-electric water purification using photocatalytic oxidation with TiO_2 as a stationary phase, Solar Energy 38 (1987) 405.
[23] N.J. Peill, M.R. Hoffmann, Development and optimization of a TiO_2-coated fibre-optic cable reactor: photocatalytic degradation of 4-chlorophenol, Environ. Sci. Technol. 29 (1995) 2974.
[24] A. Haarstrick, O.M. Kut, E. Heinzle, TiO_2-assisted degradation of environmentally relevant organic compounds in wastewater using a novel fluidized bed photoreactor, Environ. Sci. Technol. 30 (1996) 817.